Unmanned Systems, Vol. 14, No. 1 (2026) 63–77

DOI: 10.1142/S2301385025500827

UNMANNED SYSTEMS
https://www.worldscientific.com/worldscinet/us

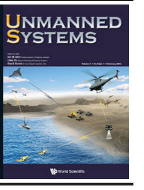

On Explicit Optimal Strategies for Two Pursuit-evasion Problems under Distance Condition in Frame of Differential Games

Zinxin Feng [*,†], Wenchao Xue [*,†,§], Hongsheng Qi [*,†], Long Cheng [‡]

[*]*School of Mathematical Sciences, University of Chinese Academy of Sciences, Beijing, P. R. China*

[†]*Academy of Mathematics and Systems Sciences, Chinese Academy of Sciences, Beijing, P. R. China*

[‡]*Institute of Automation, Chinese Academy of Sciences, Beijing, P. R. China*

This paper studies two pursuit-evasion problems under distance conditions in frame of differential game. In particular, a zero-sum differential game with the objective of distance and a nonzero-sum differential game with objective of both distance and azimuth adjustment are presented. The two players in the games are described by a nonlinear dynamics model subject to both speed and acceleration constraints in the two-dimensional plane. Instead of numerical solutions, the explicit equilibrium solutions of these two differential games are given under the condition that the distance between two players is larger than a certain value. Finally, the simulation results of these two differential games under typical cases demonstrate the effectiveness of our method.

Keywords: Pursuit-evasion (PE) problems; differential games (DGs); trajectory planning; Nash equilibria.

1. Introduction

Trajectory planning problems have received plenty of research interests for decades in many fields, such as aerospace [1, 2], autonomous vehicle [3, 4] and robotics [5]. Existing methods for trajectory planning problems include game theory [6], the optimal control approach [7], artificial potential field [8], genetic algorithm [9], simulated annealing [10], etc. Among these methods, differential game (DG) theory [11] is an effective method to tackle the trajectory planning problems.

In fact, trajectory planning in pursuit-evasion (PE) problems using DG theory have been broadly studied for decades. In [12], a complex PE game with state variable inequality constraints was investigated. The numerical solutions were obtained by multiple shooting methods. Turetsky and Shinar [13] considered a PE problem in a linear quadratic DG form, where two cases that control with and without boundary were considered and compared. Reference [14] investigated a PE game with two pursuers and one evader and the construction of the barrier that separates the state zone into capture zone and escape zone. In [15], a target defense game with two defenders and a faster intruder is solved based on the classic DG theory. Jagat and Sinclair [16] considered a spacecraft PE game and derived feedback control law using state-dependent Riccati equation method. In [17], Lin and Qu studied a PE game with multiple pursuers and one evader. The pursuers had limited observation ability and consequently they needed to cooperate in order to capture the evader. In [18], a PE game with switched linear system was investigated. Two cases of complete and incomplete information were discussed. Tang and Ye [19] investigated the problem of spacecraft interception game with incomplete information and a new game switching strategy method for spacecraft with incomplete-information is presented. In [20], a PE game with N

Received 2 July 2024; Revised 15 October 2024; Accepted 15 October 2024; Published 6 December 2024. This paper was recommended for publication in its revised form by editorial board member, Yi Dong.
Email Address: [§]*wenchaoxue@amss.ac.cn*
[§]Corresponding author.

pursuers and M evaders $(N \leq M)$ was considered and the optimal task assignment algorithm was given. Zhou and Shewchuk [21] studied so-called lion man PE problem in a closed, bounded, two-dimensional arena, which can include obstacles. In [22], a multi-agent PE game with limited sensing capabilities was investigated. A graph-theoretic approach was employed and Nash equilibrium was obtained by using the solutions of the Hamilton–Jacobi–Isaacs equations of the game. Wang and Dong [23] considered a PE problem with multiple pursuers and one evader by means of reinforcement learning. Some other learning-based methods for DGs can be found in [24, 25].

Generally speaking, there are two classes of analysis results in the existing research on PE problems. First, PE problems can use simple dynamic models, such as linear models [17, 22, 25], or models in which players have fixed speed [20, 26]. When the model is simple, the explicit strategies can usually be obtained. However, the simple dynamic models are difficult to apply in practice. Second, PE problems also can use complex kinetics [12] and the numerical solutions can be obtained [27, 28]. However, the explicit solutions of PE problems with complex kinetics are usually hard to obtain and the numerical solutions have high computational complexity. The learning-based approaches require a lot of training, which also have high computational cost. Instead of that, this paper obtains the explicit strategies of two PE games under a more practical nonlinear model. Specifically, the main contributions of this paper are summarized in the following:

- A model of PE problem is established with nonlinear kinematics. In particular, compared with the existing literature that can obtain explicit solutions but applies simpler dynamics, we use the players' normal and tangential acceleration as control inputs to establish a model of more practicality.
- The explicit equilibrium solutions for the nonzero-sum DG with the objective of distance and azimuth adjustment time (OD & AAT) are presented under distance conditions. It is proven that the equilibrium strategy of the purser can be given explicitly and the equilibrium strategy of the evader is determined by the switching time of its control input.
- The equilibrium solutions for the zero-sum DG with the OD are also presented under distance conditions. It is shown that the equilibrium strategies of both pursuer and evader are determined by the switching times of their control inputs. The simulation results under typical scenarios show the effectiveness of our methods.

The rest of this paper is organized as follows. Section 2 explains the notations used in this paper. Section 3 is on the model description and the formulation of the DGs we consider. Section 4 investigates the properties of the Nash equilibrium of these games. Section 5 shows the simulation results and Sec. 6 draws a conclusion. Besides, some lemmas and their proofs are given in the appendices.

2. Notations

In this paper, two confrontation scenarios of player 1 and player 2 on a two-dimensional plane are considered. Player 1 is the evader and player 2 is the pursuer. For the convenience of discussion, the subsequent subscripts satisfy $i \in \{1, 2\}$, $j \in \{1, 2\}$ and $i \neq j$. The following denotations are given:

(x_i, y_i): the coordinate of player i.

$\mathbf{v}_i, v_i$: the velocity vector and speed of player i, respectively. $\mathbf{v}_i \triangleq (v_{ix}, v_{iy})^T$ and $v_i = \sqrt{v_{ix}^2 + v_{iy}^2}$.

$h(x, y)$: a function to calculate the angle between a vector $(x, y)^T$ and the positive direction of x-axis.

$$h(x,y) \triangleq \begin{cases} \arctan\left(\dfrac{y}{x}\right) & \text{if } x > 0, \\ \arctan\left(\dfrac{y}{x}\right) + \pi & \text{if } x < 0 \text{ and } y > 0, \\ \arctan\left(\dfrac{y}{x}\right) - \pi & \text{if } x < 0 \text{ and } y < 0, \\ \dfrac{\pi}{2} & \text{if } x = 0 \text{ and } y > 0, \\ -\dfrac{\pi}{2} & \text{if } x = 0 \text{ and } y < 0. \end{cases}$$

θ_i: the velocity direction angle of player i. $\theta_i = h(v_{ix}, v_{iy})$.

a_{iT}, a_{iN}: the tangential and accelerations of player i. The positive direction of a_{iT} is the same with $\mathbf{v}_i$. The positive direction of a_{iN} is perpendicular to $\mathbf{v}_i$ and points to its left.

For aircraft, a_{iT} can be considered as the accelerations provided by thrust and air resistance to increase or decrease the speeds and a_{iN} can be regarded as the accelerations provided by lateral force to turn the aircraft left or right. Although using a_{iT} and a_{iN} as control inputs will make the system nonlinear, it will be closer to reality. The relation between $\mathbf{v}_i$, θ_i, a_{iT} and a_{iN} is shown in Fig. 1, where $\theta_i > 0$, $a_{iT} > 0$ and $a_{iN} > 0$.

t_0, t_f: the initial time and the terminal time.

$d(t)$: the distance between $(x_1(t), y_1(t))^T$ and $(x_2(t), y_2(t))^T$.

$\bar{d}_{ij}(t)$: the distance between $(x_i(t), y_i(t))^T$ and $(x_j(t_f), y_j(t_f))^T$, i.e. the distance between the position of player i at the current time and the position of player j at the terminal time.

Taking player 1 as an example, the difference between $d(t)$ and $\bar{d}_{12}(t)$ is shown in Fig. 2.

α_i: the real-time line-of-sight (RTLOS) angle of player i. $\alpha_i(t) \triangleq h(x_j(t) - x_i(t), y_j(t) - y_i(t))$.

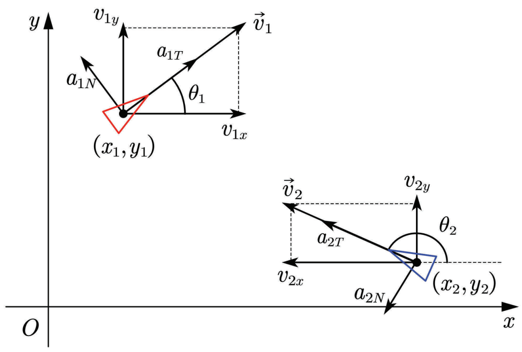

Fig. 1. The relation between $\mathbf{v}_i$, θ_i, a_{iT} and a_{iN}.

β_i: the terminal-time line-of-sight (TTLOS) angle of player i. $\beta_i(t) \triangleq h(x_j(t_f) - x_i(t), y_j(t_f) - y_i(t))$.

φ_i: the real-time azimuth (RTA), i.e. the angle between RTLOS and $\mathbf{v}_i$. φ_i satisfies

$$\varphi_i = \begin{cases} \alpha_i - \theta_i & \text{if } \alpha_i - \theta_i \in [-\pi, \pi], \\ \alpha_i - \theta_i - 2\pi & \text{if } \alpha_i - \theta_i > \pi, \\ \alpha_i - \theta_i + 2\pi & \text{if } \alpha_i - \theta_i < -\pi. \end{cases}$$

ψ_i: the terminal-time azimuth (TTA), i.e. the angle between TTLOS and $\mathbf{v}_i$. ψ_i satisfies

$$\psi_i = \begin{cases} \beta_i - \theta_i & \text{if } \beta_i - \theta_i \in [-\pi, \pi], \\ \beta_i - \theta_i - 2\pi & \text{if } \beta_i - \theta_i > \pi, \\ \beta_i - \theta_i + 2\pi & \text{if } \beta_i - \theta_i < -\pi. \end{cases}$$

Taking player 1 as an example, the difference and relationship between these real-time and terminal-time angles are illustrated in Fig. 2.

Remark 2.1. The reason why we consider the azimuth, i.e. φ_i and ψ_i, is that the range of azimuth has practical significance. For example, many players in a game, such as aircraft, can only detect targets within a certain angle range in front of themselves in the actual scenario. Besides, some airborne weapons can only achieve optimal attack effect at specified azimuth angle ranges. These detection or attack ranges can be described by the azimuth defined above.

3. Problem Formulation

The dynamics of these two players is described by the following nonlinear dynamic model:

$$\begin{cases} \dot{x}_i = v_{ix}, \\ \dot{y}_i = v_{iy}, \\ \dot{v}_{ix} = a_{iT}\cos\theta_i - a_{iN}\sin\theta_i, \\ \dot{v}_{iy} = a_{iT}\sin\theta_i + a_{iN}\cos\theta_i, \end{cases} \tag{1}$$

where both a_{iT} and a_{iN} are the strategies of player i. The state variables and strategies of player i satisfy the following constraints:

$$\begin{cases} v_i \in [\underline{v}_i, \bar{v}_i], \\ a_{iT} \in [\underline{a}_{iT}, \bar{a}_{iT}], \\ a_{iN} \in [-\bar{a}_{iN}, \bar{a}_{iN}], \end{cases} \tag{2}$$

where $\bar{v}_i > \underline{v}_i > 0$, $\bar{a}_{iT} > 0 > \underline{a}_{iT}$ and $\bar{a}_{iN} > 0$ are constants. According to the definitions of a_{iT} and a_{iN}, there hold $\dot{v}_i = a_{iT}$ and $\dot{\theta}_i = a_{iN}/v_i$. Thus we can transform the speed constraint into the acceleration constraint, i.e.

$$\begin{cases} a_{iT} \in [\underline{a}_{iT}, \bar{a}_{iT}] & \text{if } v_i \in (\underline{v}_i, \bar{v}_i), \\ a_{iT} \in [0, \bar{a}_{iT}] & \text{if } v_i = \underline{v}_i, \\ a_{iT} \in [\underline{a}_{iT}, 0] & \text{if } v_i = \bar{v}_i. \end{cases} \tag{3}$$

Equation (3) means that the player can only accelerate or keep constant speed when the speed reaches the minimum and can only decelerate or keep constant speed when the speed reaches the maximum. Then, the condition (2) can be satisfied by the following assumptions.

Assumption 3.1. a_{iT} satisfies (3) and a_{iN} satisfies

$$a_{iN} \in [-\bar{a}_{iN}, \bar{a}_{iN}].$$

Furthermore, if one wants the strategies to be physically implementable, two adjacent discontinuous points of the strategies cannot be too close in time, i.e. the strategies cannot be switched too fast. Taking this fact into account, define t_{iT}^k and t_{iN}^k, $k = 1, 2, \ldots$, as the discontinuities of a_{iT}

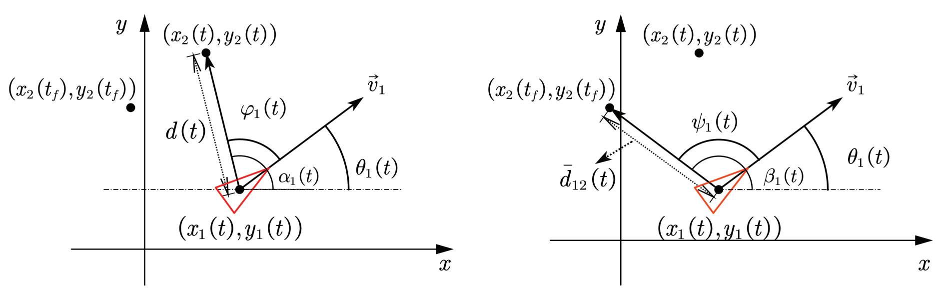

(a) The relationship between d, θ_1, α_1 and φ_1. (b) The relationship between $\bar{d}_{12}$, θ_1, β_1 and ψ_1.

Fig. 2. The difference and relationship between d, $\bar{d}_{12}$, θ_1, α_1, φ_1, β_1 and ψ_1.

and a_{iN}, respectively. Suppose the players' strategies satisfies the following assumption.

Assumption 3.2. t_{iT}^k and t_{iN}^k satisfy

$$\min_k t_{iT}^{k+1} - t_{iT}^k > \Delta_t, \quad \min_k \ t_{iN}^{k+1} - t_{iN}^k > \Delta_t,$$

where Δ_t is a constant.

Then, the admissible strategy sets are defined as follows:

$$U_{iT} \triangleq \left\{ a_{iT} \middle| \begin{array}{l} a_{iT}(t) \text{ satisfies Assumption 3.1 and} \\ \text{Assumption 3.2 for } t \in [t_0, t_f] \end{array} \right\},$$
$$U_{iN} \triangleq \left\{ a_{iN} \middle| \begin{array}{l} a_{iN}(t) \text{ satisfies Assumption 3.1 and} \\ \text{Assumption 3.2 for } t \in [t_0, t_f] \end{array} \right\}.$$

Regarding player 1 as the evader and player 2 as the pursuer, consider the following two DGs shown in Tables 1 and 2. DG with OD in Table 2 is a zero-sum game in which two players, respectively, try to maximize and minimize the distance between each other. In DG with OD & AAT in Table 1, while player 1 tries to maximize the distance from player 2, given a terminal azimuth constraint $\varphi_2(t_f) = \varphi_f$, player 2 tries to minimize the adjustment time. The reason why we consider this objective of player 2 is that the pursuer sometimes needs to adjust its attitude with respect to the evader as soon as possible to gain advantages (see Remark 2.1). For example, the pursuer will try to adjust its azimuth in order to detect the evader or launch weapons.

Then, the Nash equilibrium of a DG and the necessary conditions of the equilibrium are introduced. In general, for a nonzero-sum DG (zero-sum DG is a special case of nonzero-sum DG when $J_1 = -J_2$).

$$\begin{cases} \dot{x} = f(x, u_1, u_2), \quad x(t_0) = x_0, \\ \min\limits_{u_i} \ J_i = k_i(x(t_f)) + \displaystyle\int_{t_0}^{t_f} l_i(x, u_1, u_2) dt, \end{cases} \tag{4}$$

the Nash equilibrium is defined as follows.

Definition 3.3. The strategies of player i, $u_i^*(\cdot)$, and of player j, $u_j^*(\cdot)$ are said to be in a Nash equilibrium, if for any other admissible strategy $u_i(\cdot)$ and $u_j(\cdot)$, the following inequality holds:

$$J_i(u_i^*, u_j^*) \le J_i(u_i, u_j^*),$$
$$J_j(u_i^*, u_j^*) \le J_j(u_i^*, u_j).$$

Table 1. DG with objective of distance and azimuth adjustment time (OD & AAT).

Optimization objective	$\max_{a_{1T}, a_{1N}} d(t_f)$, $\min_{a_{2T}, a_{2N}} t_f$
State equations	(1) for $i = 1, 2$
Admissible strategies set	U_{iT} and U_{iN} for $i = 1, 2$
Terminal constraint	$\varphi_2(t_f) = \varphi_f$
Remark	The terminal time is free

Table 2. DG with OD

Optimization objective	$\max_{a_{1T}, a_{1N}} \min_{a_{2T}, a_{2N}} d(t_f)$
State equations	(1) for $i = 1, 2$
Admissible strategies set	U_{iT} and U_{iN} for $i = 1, 2$
Remark	The terminal time is fixed

The authors of [29] and [30] present the necessary conditions for the Nash equilibrium of a nonzero-sum DG. If the trajectory corresponding to (u_1^*, u_2^*) is x^* and Hamiltonian is

$$H_i = -l_i(x, u_1, u_2) + \lambda_i^T \cdot f(x, u_1, u_2),$$

then λ_i, x^* and u_i^* must satisfy

$$\begin{cases} \dot{\lambda}_i = -\partial H_i(x^*, u_1^*, u_2^*, \lambda_i)/\partial x, \\ \lambda_i(t_f) = -\partial k_i(x^*(t_f))/\partial x, \\ u_i^* = \arg\max\limits_{u_i} H_i(x^*, u_i, u_j^*, \lambda_i). \end{cases} \tag{5}$$

However, it is quite difficult to obtain the optimal strategies for the DG in Tables 1 and 2 by using the necessary conditions directly because it needs to solve two-point boundary value problems. Instead of that, we will show the properties of the equilibrium strategies of these two problems under some certain conditions in the following section.

4. Main Results

4.1. *Explicit solutions of DG with OD & AAT*

Suppose the equilibrium solutions of DG in Table 1 are a_{iT}^* and a_{iN}^*. Theorem 4.1 provides the properties of a_{1T}^* and a_{1N}^*.

Theorem 4.1. *Consider the DG with OD & AAT in Table* 1. *Let*

$$\bar{d}_{12}(t) > \bar{v}_1(t_f - t_0) \max\left\{ \frac{1}{|\psi_1(t_0)|}, \frac{2\bar{v}_1}{\bar{a}_{1N}\Delta_t} \right\} \tag{6}$$

holds. Then, a_{1T}^* and a_{1N}^* satisfy

$$a_{1T}^*(t) = \begin{cases} \underline{a}_{1T} & \text{if } v_1 \in (\underline{v}_1, \bar{v}_1] \text{ and } t \in [t_0, t_{s_1}), \\ 0 & \text{if } v_1 = \underline{v}_1 \text{ and } t \in [t_0, t_{s_1}), \\ \bar{a}_{1T} & \text{if } v_1 \in [\underline{v}_1, \bar{v}_1) \text{ and } t \in [t_{s_1}, t_f], \\ 0 & \text{if } v_1 = \bar{v}_1 \text{ and } t \in [t_{s_1}, t_f], \end{cases} \tag{7}$$

$$a_{1N}^*(t) = \begin{cases} -\mathrm{sign}(\psi_1(t_0))\bar{a}_{1N} & \text{if } |\psi_1(t)| < \pi, \\ 0 & \text{if } |\psi_1(t)| = \pi, \end{cases} \tag{8}$$

where t_{s_1} is an undetermined time and $t_{s_1} \in [t_0, t_f]$.

The proof of Theorem 4.1 is in Appendix A.

Remark 4.2. Equation (7) indicates that when $t \in [t_0, t_{s_1})$, player 1 should decelerate if its speed did not reach the lower bound $\underline{v}_1$, otherwise maintain the speed at $\underline{v}_1$. In other words, player 1 should minimize v_1 when $t \in [t_0, t_{s_1})$. Similarly, player 1 should maximize v_1 when $t \in [t_{s_1}, t_f]$. Equation (8) shows that the equilibrium strategy for a_{1N} is to turn round with maximum normal acceleration until $|\psi_1| = \pi$ and then keeps $|\psi_1| \equiv \pi$, i.e. player 1 (the evader) keeps moving with its back to player 2.

Next, we will discuss the equilibrium strategies for the pursuer with azimuth adjustment objective. For the convenience of subsequent discussion, we define $A_{2T} = \max\{\bar{a}_{2T}, |\underline{a}_{2T}|\}$ and

$$\eta_2(t) = \begin{cases} \varphi_2(t) - \varphi_f & \text{if } \varphi_2(t) - \varphi_f \in [-\pi, \pi], \\ \varphi_2(t) - \varphi_f + 2\pi & \text{if } \varphi_2(t) - \varphi_f < -\pi, \\ \varphi_2(t) - \varphi_f - 2\pi & \text{if } \varphi_2(t) - \varphi_f > \pi, \end{cases}$$

where $\eta_2 \in [-\pi, \pi]$ represents the gap between current TTA and desired TTA. The constraint $\varphi_2(t_f) = \varphi_f$ is equivalent to $\eta_2(t_f) = 0$.

Then, Theorem 4.3 shows the explicit equilibrium strategies of player 2 in DG with OD & AAT.

Theorem 4.3. *Consider DG with OD & AAT in Table 1. Let*

$$d(t) > \max\left\{\sqrt{2}(\bar{v}_1 + \bar{v}_2)\frac{t_f - t_0}{\pi - |\eta_2(t_0)|}\right.$$
$$\left.\bar{v}_2 \exp\left(\frac{A_{2T}}{\underline{v}_2}(t_f - t)\right)\left(\frac{\bar{v}_2}{\bar{a}_{2N}} + t_f - t\right)\right\}, \tag{9}$$

holds. Then

$$a_{2T}^* = \begin{cases} \underline{a}_{2T} & \text{if } v_2 \in (\underline{v}_2, \bar{v}_2], \\ 0 & \text{if } v_2 = \underline{v}_2, \end{cases} \tag{10}$$

$$a_{2N}^*(t) = \mathrm{sign}(\eta_2(t_0))\bar{a}_{2N}. \tag{11}$$

The proof of Theorem 4.1 is in Appendix B.

Remark 4.4. The equilibrium solutions given in Theorem 4.1 and Theorem 4.3 require the distance between two players to be larger than a certain value. In practice, many scenarios need to consider the manoeuvring strategies under such distance conditions due to the large detection range (compared to the speed of the player) of existing radar.

4.2. *Explicit solutions of DG with OD*

Suppose the equilibrium solutions of DG in Table 2 are a_{iT}^* and a_{iN}^*, which can be obtained by the following two theorems

Theorem 4.5. *Consider the DG with OD. Let (6) hold, then, a_{1T}^* and a_{1N}^* are exactly the same as Theorem 4.1.*

Theorem 4.6. *Consider the DG with OD in Table 2. Let*

$$\bar{d}_{21}(t) > \bar{v}_2(t_f - t_0)\max\left\{\frac{1}{\pi - |\psi_2(t_0)|}, \frac{2\bar{v}_2}{\bar{a}_{2N}\Delta_t}\right\}.$$

Then, a_{2T}^* and a_{2N}^* satisfy

$$a_{2T}^*(t) = \begin{cases} \underline{a}_{2T} & \text{if } v_2 \in (\underline{v}_2, \bar{v}_2] \text{ and } t \in [t_0, t_{s_2}), \\ 0 & \text{if } v_2 = \underline{v}_2 \text{ and } t \in [t_0, t_{s_2}), \\ 0 & \text{if } v_2 = \bar{v}_2 \text{ and } t \in [t_{s_2}, t_f], \\ \bar{a}_{2T} & \text{if } v_2 \in [\underline{v}_2, \bar{v}_2) \text{ and } t \in [t_{s_2}, t_f], \end{cases}$$

$$a_{2N}^*(t) = \begin{cases} \mathrm{sign}(\psi_2(t_0))\bar{a}_{2N} & \text{if } |\psi_2(t)| > 0, \\ 0 & \text{if } |\psi_2(t)| = 0, \end{cases}$$

where $t_{s_2} \in [t_0, t_f]$ is an undetermined time.

Proof of Theorem 4.5 and 4.6. Theorem 4.5can be proven in exactly the same way as Theorem 4.1. Consider Theorem 4.6. Due to the performance index of player 2 in DG with OD (see Table 2) is minimization instead of maximization, the sign of a_{2T}^* and a_{2N}^* should be the same as the sign of theirs coefficients in the Hamiltonian, while the sign of a_{1T}^* and a_{1N}^* should be opposite to the sign of theirs coefficients in the Hamiltonian. Taking this into account, the rest of the proof of Theorem 4.6 is similar to the proof of Theorem 4.1 □

Remark 4.7. Note that the only opponent's information required in the proposed strategies is positions, which are used to calculate some relevant angles.

Remark 4.8. The intuitive understanding of the distance conditions in theorems is that they allow a relatively long distance between two players, which reduces the impact of opponents' decisions on the player. Similarly, the distance conditions will also reduce the influence of observation errors on the problems, which will be explained in Sec. 5.3.

5. Cases Study

In this section, numerical solutions for special cases are given to verify validity of the theoretical results. According to Definition 3.3, given a pair of strategies (u_1^*, u_2^*), one can solve the following two optimal control problems (OCPs) to validate that (u_1^*, u_2^*) is the equilibrium solution of DG (4).

$$\begin{cases} \dot{x} = f(x, u_1, u_2^*), \quad x(t_0) = x_0, \\ \min\limits_{u_1} J_1 = k_1(x(t_f)) + \displaystyle\int_{t_0}^{t_f} l_1(x, u_1, u_2^*)dt, \end{cases} \tag{12}$$

Table 3. Simulation setup.

Parameters	Values
$(x_1(t_0), y_1(t_0))$	(0,0) m
$(x_2(t_0), y_2(t_0))$	(1000,0) m
$(v_{1x}(t_0), v_{1y}(t_0))$	(10,10) m/s
$(v_{2x}(t_0), v_{2y}(t_0))$ in DG with OD & AAT	(0,30) m/s
$(v_{2x}(t_0), v_{2y}(t_0))$ in DG with OD	(0,10) m/s
$\underline{v}_i$, $\bar{v}_i$	10 m/s, 40 m/s
$\underline{a}_{iT}$, $\bar{a}_{iT}$	-3 m/s^2, 4 m/s^2
$\bar{a}_{iN}$	5 m/s^2
φ_f	30°
t_0	0 s
t_f of DG with OD	10 s

$$\begin{cases} \dot{x} = f(x, u_1^*, u_2), \quad x(t_0) = x_0, \\ \min\limits_{u_2} J_2 = k_2(x(t_f)) + \displaystyle\int_{t_0}^{t_f} l_2(x, u_1^*, u_2)dt. \end{cases} \tag{13}$$

Specifically, suppose the solutions of (12) and (13) are u_1' and u_2', respectively. If $u_1' = u_1^*$ and $u_2' = u_2^*$, then (u_1^*, u_2^*) is exactly the Nash equilibrium. Numerical solutions of the OCPs are obtained by a MATLAB software, GPOPS, using a pseudospectral method. The parameters used in this section are listed in Table 3.

5.1. *Simulation results of DG with OD & AAT*

The explicit expressions of a_{2T}^* and a_{2N}^* are already obtained in Theorem 4.3. Note that TTA, $\psi_1(t)$, needs the terminal position of player 2, which is difficult to obtain at the initial time. For implementation, one can replace $\psi_1(t)$

Algorithm 5.2. Iterative Algorithm Based on Explicit Expressions (IABEE)

Initialization: Initial strategy of player 1, (a_{1T}^0, a_{1N}^0). Set $k = 1$ and tolerance error $\varepsilon > 0$.
Step 1: Player 1 obtains trajectory X_1^k by (a_{1T}^k, a_{1N}^k).
Step 2: Player 2 obtains $(a_{2T}^{k+1}, a_{2N}^{k+1})$ from Theorem 4.3 according to X_1^{k+1}.
Step 3: Player 2 obtains trajectory X_2^{k+1} by $(a_{2T}^{k+1}, a_{2N}^{k+1})$.
Step 4: Player 1 obtains $(a_{1T}^{k+1}, a_{1N}^{k+1})$ from Theorem 4.1 according to X_2^{k+1}.
Step 5:
If $\forall t > 0$, $|a_{iT}^{k+1} - a_{iT}^k| < \varepsilon$ and $|a_{iN}^{k+1} - a_{iN}^k| < \varepsilon$, **then**
  Stop and **return** $(a_{iT}^{k+1}, a_{iN}^{k+1})$.
Else
  $k = k + 1$ and go back to **Step 1.**

---

with RTA, $\varphi_1(t)$, in (8) to get an approximate equilibrium strategy under the distance condition. In fact, $|\psi_1(t) - \varphi_1(t)|$ is small enough when distance conditions hold, which can be obtained by the following proposition.

Proposition 5.1. *If $d(t) > \bar{v}_j(t_f - t)$, then the error between $\varphi_i(t)$ and $\psi_i(t)$ satisfies*

$$|\psi_i(t) - \varphi_i(t)| \le \left| arcsin\frac{\bar{v}_j(t_f - t)}{d(t)} \right|. \tag{14}$$

Proposition 5.1 is proved in Appendix E.

As for a_{1T}^*, according to Theorem 4.1, t_{s_1} can be determined by discretizing the time interval and using the traversal method to find the time that makes objective optimal. Then, we use a iterative algorithm based on explicit

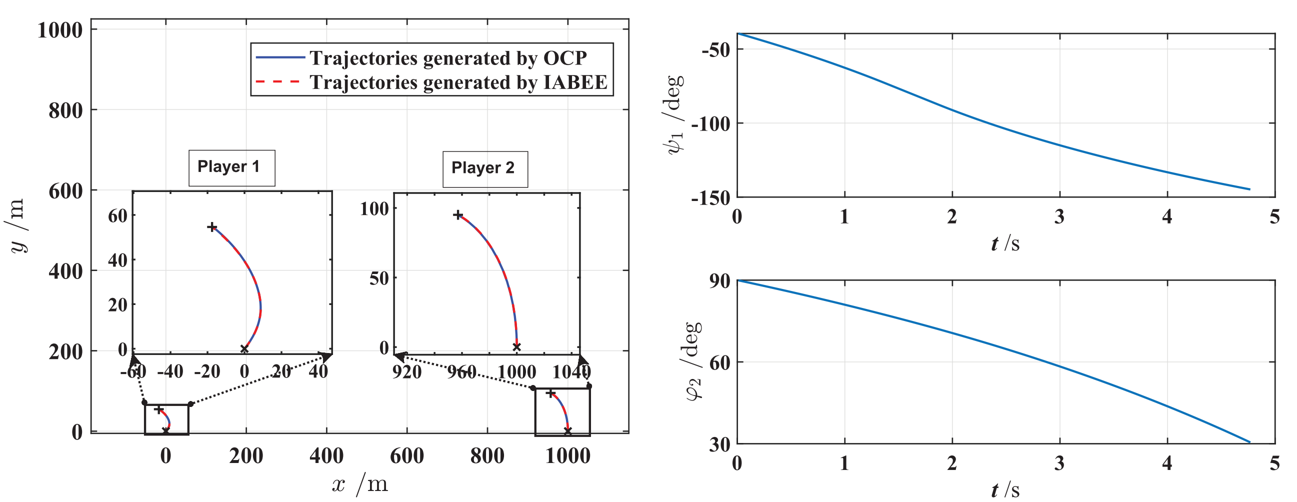

(a) The trajectories of two players.

(b) The azimuths of two players.

Fig. 3. Simulation results of DG with OD & AAT.

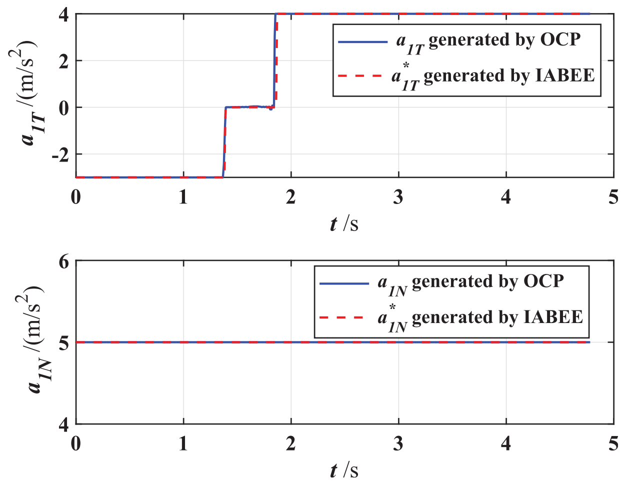

(c) The strategy of player 1.

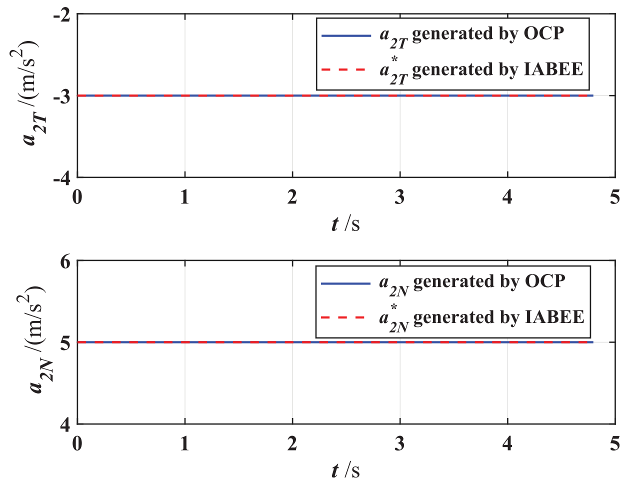

(d) The strategy of player 2.

Fig. 3. (*Continued*)

expression (IABEE) shown below to obtain equilibrium solutions (a^*_{iT}, a^*_{iN}).

After generating (a^*_{iT}, a^*_{iN}) by IABEE, two OCPs, i.e. Eqs. (12) and (13), are solved and compared to validate (a^*_{iT}, a^*_{iN}) is exactly the Nash equilibrium. The simulation and comparison results are shown in Fig. 3.

From Fig. 3, one can see that the optimal solutions of the OCPs and the equilibrium solutions generated by Theorems 4.1 and 4.3 approximately coincide. Figure 3(b) shows that player 2 in DG with OD & AAT has reached its expected RTA ($\varphi_f = 30°$) which indicates the effectiveness of (7), (8), (10) and (11). Note that player 2's equilibrium solution and the solution from OCP are exactly the same because Theorem 4.3 gives directly the explicit expressions of a^*_{2T} and a^*_{2N}.

5.2. *Simulation results of DG with OD*

In this section, we also use IABEE to obtain the equilibrium solutions, except that (a^*_{1T}, a^*_{1N}) and (a^*_{2T}, a^*_{2N}) are obtained from Theorems 4.5 and 4.6, respectively.

The simulation and comparison results of DG with OD are shown in Fig. 4. From Fig. 4, although both player 1 and

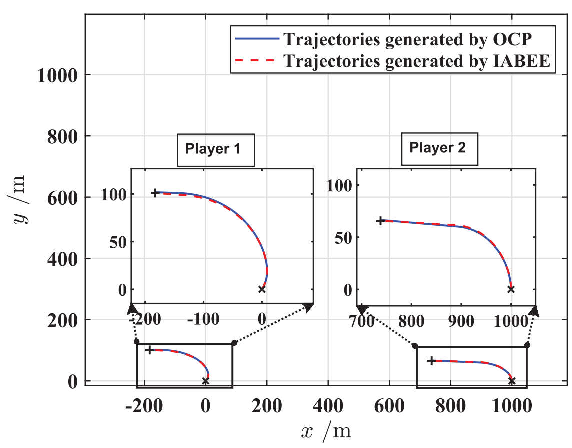

(a) The trajectories of two players.

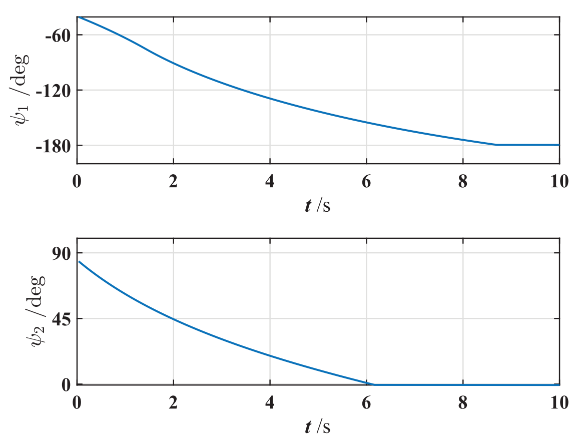

(b) The azimuths of two player.

Fig. 4. Simulation results of DG with OD.

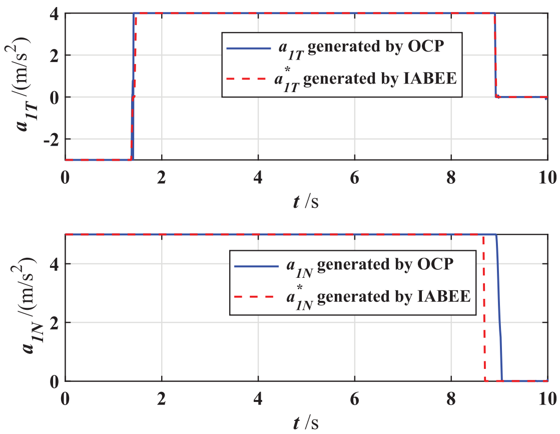

(c) The strategy of player 1.

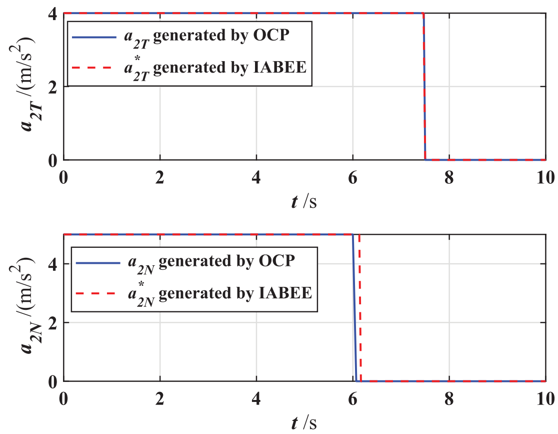

(d) The strategy of player 2.

Fig. 4. (*Continued*)

Table 4. Objective of DG with OD & AAT under different conditions.

	Without observation error		With observation error	
	Player 1	Player 2	Player 1	Player 2
$\theta_1(t_0) = 45^\circ$ $\theta_2(t_0) = 90^\circ$	975.5 m	4.78 s	975.3 m	4.75 s
$\theta_1(t_0) = 0^\circ$ $\theta_2(t_0) = 90^\circ$	937.1 m	4.84 s	939.4 m	4.78 s
$\theta_1(t_0) = 45^\circ$ $\theta_2(t_0) = 45^\circ$	1087.6 m	6.74 s	1087.2 m	6.72 s

player 2 use approximate method to get explicit equilibrium strategies, the optimal solutions of the OCPs and the equilibrium solutions generated by IABEE approximately coincide.

5.3. *Algorithm robustness analysis*

In this section, we investigate the impact of different initial conditions on algorithm results. While keeping other conditions unchanged compared to parameters in Table 3, Table 4 presents objective values of DG with OD & AAT under different initial velocity direction angles and under the scenarios where random disturbances are added to observations at the opponent's position, following a normal distribution with a mean of 0 and a standard deviation of 8. It implies that while being insensitive to disturbances, the performance is greatly affected by initial velocity direction.

6. Conclusions

This paper studies two PE problems with distance objective and AAT objective using the DG method. The equilibrium strategies are given explicitly under certain distance conditions without complicated calculations. In order to demonstrate the validity of the theoretical results, the numerical solutions of these optimal control problems are solved and confirm the effectiveness of our equilibrium strategies. In the future, the scenarios with multi-pursuer and multi-evader will be further studied.

Acknowledgments

This work was supported by the National Key R&D Program of China (No. 2022YFA1004703), the National Natural Science Foundation of China (No. 62122083), and Chinese Academy of Sciences Youth Innovation Promotion Association (No. 2021003).

Appendix A

Proof of theorem 4.1

In order to prove Theorem 4.1, two lemmas and their proofs are introduced in Appendices C and D, respectively.

First, consider the Hamiltonian of player 1 in this problem, i.e.

$$\begin{aligned} H_1 = {} & \lambda_{11} v_{1x} + \lambda_{12} v_{1y} + \lambda_{13}(a_{1T}\cos\theta_1 - a_{1N}\sin\theta_1) \\ & + \lambda_{14}(a_{1T}\sin\theta_1 + a_{1N}\cos\theta_1) \\ & + \lambda_{15} v_{2x} + \lambda_{16} v_{2y} + \lambda_{17}(a_{2T}\cos\theta_2 - a_{2N}\sin\theta_2) \\ & + \lambda_{18}(a_{2T}\sin\theta_2 + a_{2N}\cos\theta_2), \end{aligned} \tag{A.1}$$

where $\lambda_{1k}, k = 1, \ldots, 8$ represent the components of co-state of player 1, i.e. λ_1. Let $f_1(t)$ and $g_1(t)$ represent the coefficients of a_{1T} and a_{1N} in the Hamiltonian, respectively, i.e.

$$\begin{aligned} f_1(t) &= \lambda_{13}\cos\theta_1 + \lambda_{14}\sin\theta_1, \\ g_1(t) &= -\lambda_{13}\sin\theta_1 + \lambda_{14}\cos\theta_1. \end{aligned}$$

Since the performance index of player 1 in DG with OD & AAT is maximization instead of minimization, according to (5), one can easily obtain that if $f_1(t) > 0$, then $a^*_{1T}(t)$ takes value at the lower bound of (3); if $f_1(t) < 0$, then $a^*_{1T}(t)$ takes value at the upper bound of (3). $a^*_{1N}(t)$ have similar results about $g_1(t)$.

Besides, according to (5), $\dot\lambda_{11} = -\partial H_1/\partial x_1 = 0$ and $\lambda_{11}(t_f) = -\partial d(t_f)/\partial x_1 = -\partial \bar d_{12}(t_f)/\partial x_1 = \cos\beta_1(t_f)$. Thus $\lambda_{11}(t) \equiv \cos\beta_1(t_f)$. Similarly we have $\lambda_{12}(t) \equiv \sin\beta_1(t_f)$. For λ_{13}, one can obtain that $\lambda_{13}(t_f) = -\partial d(t_f)/\partial v_{1x} = 0$ and

$$\begin{aligned} \dot\lambda_{13}(t) &= -\frac{\partial H_1}{\partial v_{1x}} \\ &= -\lambda_{11} - \frac{\partial \cos\theta_1}{\partial v_{1x}}(\lambda_{13}a_{1T} + \lambda_{14}a_{1N}) \\ &\quad - \frac{\partial \sin\theta_1}{\partial v_{1x}}(-\lambda_{13}a_{1N} + \lambda_{14}a_{1T}), \end{aligned} \tag{A.2}$$

$$\frac{\partial \sin\theta_1}{\partial v_{1x}} = -\cos\theta_1\sin\theta_1\frac{1}{v_1}. \tag{A.3}$$

$$\begin{aligned} \frac{\partial \cos\theta_1}{\partial v_{1x}} &= -\sin\theta_1\frac{\partial}{\partial v_{1x}}\left(\arctan\frac{v_{1y}}{v_{1x}}\right) \\ &= \sin^2\theta_1\frac{1}{v_1}, \end{aligned} \tag{A.4}$$

By substituting (A.4) and (A.3) into (A.2), we have

$$\begin{aligned} \dot\lambda_{13} = {} & -\cos\beta_1(t_f) - (\lambda_{13}a_{1T} + \lambda_{14}a_{1N})\frac{\sin^2\theta_1}{v_1}, \\ & + (-\lambda_{13}a_{1N} + \lambda_{14}a_{1T})\frac{\cos\theta_1\sin\theta_1}{v_1}. \end{aligned} \tag{A.5}$$

Similarly, $\lambda_{14}(t_f) = 0$ and

$$\begin{aligned} \dot\lambda_{14} = {} & -\sin\beta_1(t_f) + (\lambda_{13}a_{1T} + \lambda_{14}a_{1N})\frac{\cos\theta_1\sin\theta_1}{v_1} \\ & - (-\lambda_{13}a_{1N} + \lambda_{14}a_{1T})\frac{\cos^2\theta_1}{v_1}. \end{aligned} \tag{A.6}$$

Thus $f_1(t_f) = g_1(t_f) = 0$. By taking the derivative of $f_1(t)$ and $g_1(t)$ with respect to time, substituting (A.5), (A.6) and $\dot\theta_1 = a_{1N}/v_1$, it yields that

$$\dot f_1 = -\cos(\theta_1 - \beta_1(t_f)) + g_1(t)\frac{a_{1N}}{v_1}, \tag{A.7}$$

$$\dot g_1 = \sin(\theta_1 - \beta_1(t_f)) - g_1(t)\frac{a_{1T}}{v_1}. \tag{A.8}$$

Second, set

$$U'_{1N} = \{a_{1N} | a_{1N}(t) = \pm\bar a_{1N} \text{ or } 0. \text{ And } a_{1N}(t) \in U_{1N}\}.$$

We will prove that $a^*_{1N} \in U'_{1N}$, $a_{1N}(t) \equiv \bar a_N$ decreases $\psi_1(t_0)$ to $\psi_1(t) = -\pi$ fastest and $a_{1N}(t) \equiv -\bar a_N$ increases $\psi_1(t_0)$ to $\psi_1(t) = \pi$ fastest among all of strategies belonging to U'_{1N}.

One can obtain that $a^*_{1N}(t) \in U'_{1N}$. In fact, ignoring the isolated zero points of $g_1(t)$, $a_{1N}(t) = \pm\bar a_{1N}$ when $g_1(t) \neq 0$. Suppose there exists a time interval $[t', t''] \subseteq [t_0, t_f]$ such that $g_1(t) \equiv 0$. Thus $\dot g_1(t) = g_1(t) = 0$. Note that (A.8) holds. As a result, $\sin(\theta_1 - \beta_1(t_f)) \equiv 0$, $\dot\theta_1(t) \equiv 0$ and $a_{1N}(t) = 0$ for $t \in [t', t'']$ because $\dot\theta_1 = a_{1N}/v_1$. Thus $a^*_{1N}(t) \in U'_{1N}$.

Suppose t_1 is the first time that satisfies $\psi_1(t_1) = \pi$ (if it exists, otherwise $t_1 = t_f$). It follows immediately from Lemma C.1 (shown in Appendix C) that for $t \in [t_1, t_f]$, $\psi_1(t) = \pi$ under $a^*_{1N}(t)$. That means $a^*_{1N}(t) = 0$ for $t \in [t_1, t_f]$ because it makes $\dot\psi_1 \equiv 0$ when $\psi_1(t) = \pi$. Let

$$\begin{aligned} \hat a_{1N}(t) &\equiv -\bar a_{1N}, t \in [t_0, t_1], \\ \hat a'_{1N}(t) &= \begin{cases} \hat a_{1N}(t) & \text{if } t \in [t_0, t_2) \cap (t_2 + \Delta_{t_2}, t_1], \\ \bar a_{1N} & \text{if } t \in [t_2, t_2 + \Delta_{t_2}], \end{cases} \\ u_1(t) &= (a_{1T}(t), \hat a_{1N}(t))^T, \\ u'_1(t) &= (a_{1T}(t), \hat a'_{1N}(t))^T, \end{aligned}$$

where t_2 is any fixed time in $[t_0, t_1 - \Delta_{t_2}]$ and $a_{1T}(t)$ is any admissible strategy belonging to U_{1T}. Δ_{t_2} denotes the length of changed interval and $\Delta_{t_2} \geq \Delta_t$ because of the definition of U_{1N}. It is easy to get that the trajectories under $u_1(t)$ and $u'_1(t)$ have the same speed and we denote it as $v_1(t)$ for convenience.

Let $\psi_1(t)$ and $\psi'_1(t)$ be the TTAs corresponding to u_1 and u'_1, respectively. From (6), $\exists\varepsilon > 0$, s.t.

$$\frac{\bar v_1}{\bar d_{12}(t)} < \varepsilon < 2\frac{\Delta_t}{t_f - t_0}\frac{\bar a_{1N}}{\bar v_1}. \tag{A.9}$$

According to Lemma D.1 (shown in the Appendix D), $|\dot{\beta}_1| < \varepsilon$. Obviously, $\psi_1(t) \equiv \psi_1'(t)$ when $t \in [t_0, t_2)$. Consider the interval $[t_2, t_1]$. Since $\dot{\psi}_i = \dot{\beta}_i - \dot{\theta}_i$, there holds that

$$-\varepsilon + \frac{\bar{a}_{1N}}{v_1(t)} < \dot{\psi}_1(t) < \varepsilon + \frac{\bar{a}_{1N}}{v_1(t)},$$

$$-\varepsilon - \frac{\bar{a}_{1N}}{v_1(t)} < \dot{\psi}_1'(t) < \varepsilon - \frac{\bar{a}_{1N}}{v_1(t)},$$

when $t \in [t_2, t_2 + \Delta_{t_2}]$ and

$$-\varepsilon + \frac{\bar{a}_{1N}}{v_1(t)} < \dot{\psi}_1(t), \dot{\psi}_1'(t) < \varepsilon + \frac{\bar{a}_{1N}}{v_1(t)},$$

when $t \in [t_2 + \Delta_{t_2}, t_1]$. Then, for $t \in [t_2 + \Delta_{t_2}, t_1]$,

$$\begin{aligned}\psi_1(t) = & \int_{t_2}^{t} \dot{\psi}_1(\tau) d\tau + \psi_1(t_2) \\ & > \bar{a}_{1N} \int_{t_2}^{t} \frac{1}{v_1(\tau)} d\tau - \varepsilon(t - t_2) + \psi_1(t_2),\end{aligned}$$

$$\begin{aligned}\psi_1'(t) = & \int_{t_2}^{t_2+\Delta_{t_2}} + \int_{t_2+\Delta_{t_2}}^{t} \dot{\psi}_1'(\tau) d\tau + \psi_1'(t_2) \\ & < -\bar{a}_{1N} \int_{t_2}^{t_2+\Delta_{t_2}} \frac{d\tau}{v_1(\tau)} + \varepsilon \Delta_{t_2} \\ & + \bar{a}_{1N} \int_{t_2+\Delta_{t_2}}^{t} \frac{d\tau}{v_1(\tau)} + \varepsilon(t - t_2 - \Delta_{t_2}) + \psi_1'(t_2),\end{aligned}$$

$$\begin{aligned}\psi_1(t) - \psi_1'(t) & > 2\bar{a}_{1N} \int_{t_2}^{t_2+\Delta_{t_2}} \frac{d\tau}{v_1(\tau)} - 2\varepsilon(t - t_2) \\ & > 2\bar{a}_{1N} \frac{\Delta_t}{\bar{v}_1} - 2\varepsilon(t_f - t_0). \end{aligned} \tag{A.10}$$

From (A.9) and (A.10), we have $\psi_1(t) - \psi_1'(t) > 0$. Similarly, it can be proved that if

$$\hat{a}'_{1N}(t) = \begin{cases} \hat{a}_{1N}(t) & \text{if } t \in [t_0, t_2) \cap (t_2 + \Delta_{t_2}, t_1], \\ 0 & \text{if } t \in [t_2, t_2 + \Delta_{t_2}], \end{cases}$$

then $\psi_1(t) - \psi_1'(t) > 0$ also holds. That means if we make a small deviation belonging to U'_{1N} from $\hat{a}_{1N}(t)$, then $\hat{a}_{1N}(t)$ increases $\psi_1(t_0)$ to $\psi_1(t) = \pi$ the fastest. Similarly, one can prove that $a_{1N}(t) = \bar{a}_{1N}$ decreases $\psi_1(t_0)$ to $\psi_1(t) = -\pi$ the fastest.

Third, we prove the equilibrium strategy of $a_{1N}(t)$ is (8). Note the relationship between $\bar{d}_{ij}(t)$ and $\psi_i(t)$ revealed in Lemma C.1. If we can prove $a_{1N}(t) = -\bar{a}_{1N}$ increase $|\psi_1(t_0)|$ to $|\psi_1(t)| = \pi$ faster than $a_{1N}(t) = \bar{a}_{1N}$ when $\psi_1(t_0) > 0$ and $a_{1N}(t) = \bar{a}_{1N}$ increase $|\psi_1(t_0)|$ to $|\psi_1(t)| = \pi$ faster than $a_{1N}(t) = -\bar{a}_{1N}$ when $\psi_1(t_0) < 0$, then the equilibrium strategy of $a_{1N}(t)$ is exactly (8).

Take $\psi_1(t_0) = \psi_0 > 0$ as an example. In fact, from (6), $\exists \varepsilon' > 0$, s.t.

$$\frac{\bar{v}_1}{\bar{d}_{12}(t)} < \varepsilon' < \frac{\psi_0}{t_f - t_0}. \tag{A.11}$$

Denote ψ_1 and ψ_1'' as the TTAs when $a_{1N}(t) \equiv -\bar{a}_{1N}$ and $a_{1N}(t) \equiv \bar{a}_{1N}$, respectively. They satisfy

$$-\varepsilon' + \frac{\bar{a}_{1N}}{v_1(t)} < \dot{\psi}_1(t) < \varepsilon' + \frac{\bar{a}_{1N}}{v_1(t)}, \tag{A.12}$$

$$-\varepsilon' - \frac{\bar{a}_{1N}}{v_1(t)} < \dot{\psi}_1''(t) < \varepsilon' - \frac{\bar{a}_{1N}}{v_1(t)} \tag{A.13}$$

and $\psi_1(t_0) = \psi_1''(t_0) = \psi_0 > 0$, which means ψ_1 increases from ψ_0 to π and ψ_1'' decreases from ψ_0 to $-\pi$. Let $\Delta_{\dot{\psi}_1} = |\dot{\psi}_1''(t)| - |\dot{\psi}_1(t)|$. From (A.12) and (A.13), $\Delta_{\dot{\psi}_1} < 2\varepsilon'$. However, there holds

$$\begin{aligned}|-\pi - \psi_1''(t_0)| - |\pi - \psi_1(t_0)| = 2\psi_0 & \\ > (t_f - t_0) \cdot 2\varepsilon' & \\ > (t_f - t_0) \Delta_{\dot{\psi}_1}. &\end{aligned}$$

It implies that $a_{1N}(t) = -\bar{a}_{1N}$ increase $|\psi_1(t)|$ to π faster than $a_{1N}(t) = \bar{a}_{1N}$ when $\psi_1(t_0) > 0$. Similarly, one can obtain $a_{1N}(t) = \bar{a}_{1N}$ increase $|\psi_1(t)|$ to π faster than $a_{1N}(t) = -\bar{a}_{1N}$ when $\psi_1(t_0) < 0$. Furthermore, $a_{1N}(t) = 0$ makes $|\psi_1(t)| \equiv \pi$ when $|\psi_1(t)| = \pi$. Thus, (8) is exactly the equilibrium strategy of a_{1N} according to Lemma C.1.

Fourth, we prove a_{1T}^* is (7). By taking derivatives of (A.7) and substituting (8) into it, one can obtain that

$$\ddot{f}_1 = 2\dot{g}_1 \frac{a_{1N}^*}{v_1}. \tag{A.14}$$

Taking $\psi_1(t_0) = \psi_0 > 0$ as an example, it can be proved that there does not exist $t' \in [t_0, t_f]$ s.t. $f_1(t') = 0$ and $\dot{f}_1(t') > 0$. In other words, $f_1(t)$ cannot cross the x-axis from below to above.

In fact, suppose there exists $t' \in [t_0, t_f]$, s.t. $f_1(t') = 0$ and $\dot{f}_1(t') > 0$. When $\psi_1(t_0) = \psi_0 > 0$, it can be obtained from the third step that $\forall t \in [t_0, t_f]$, $g_1(t) \geq 0$, $a_{1N}^*(t) \leq 0$ and ψ_1 increases from $\psi_0 > 0$ to π (if t_f is large enough). Note (A.11), $|\beta_1(t) - \beta_1(t_f)| < \varepsilon(t_f - t_0) < \psi_0$ and

$$\theta_1 - \beta_1(t_f) = -\psi_1(t) + \beta_1(t) - \beta_1(t_f).$$

As a result, $\theta_1 - \beta_1(t_f)$ is less than 0 at t_0 and decreases monotonically with time. Thus $\sin(\theta_1 - \beta_1(t_f)) < 0$ and $-\cos(\theta_1 - \beta_1(t_f))$ increases monotonically with time.

Consider the sign of f_1, $\dot{f}_1$, $\ddot{f}_1$, g_1 and $\dot{g}_1$ in the neighborhood of t', i.e. $(t'-\delta, t'+\delta)$, δ' is small enough. $\forall t \in (t', t'+\delta)$, it can be proved that $\dot{f}_1 > 0$, $\dot{g}_1 < 0$ and $a^*_{1N} \leq 0$. From (A.14), $\ddot{f}_1 \geq 0$, $\forall t \in (t, t'+\delta)$. In addition, $\forall t \in (t, t'+\delta)$, $f_1 > 0$, $\dot{f}_1 > 0$. Therefore, f_1 will keep increasing and then $a_{1T} \leq 0$, $\dot{g}_1 < 0$, $\ddot{f}_1 > 0$, $\dot{f}_1 > 0, \ldots$ As a result, f_1 monotonic increases in $(t', t_f]$. However, $f_1(t') = f_1(t_f) = 0$. This leads to contradiction, which means that there does not exist a time $t' \in [t_0, t_f]$, s.t. $f_1(t') = 0$ and $\dot{f}_1(t') > 0$.

Note that $\dot{f}_1$ exists and therefore f_1 is continuous. Consequently, there are only three cases of $f_1(t)$: $f_1(t) > 0$, $f_1(t) < 0$ or $f_1(t)$ is first greater than 0 and then less than 0. Suppose t_{s_1} is the time that f_1 crosses x-axis from above to below (let $t_{s_1} = t_f$ in the first case and $t_{s_1} = t_0$ in the second case). Then a^*_{1T} takes value at the lower bound for $t \in [t_0, t_{s_1})$ and a^*_{1T} takes value at the upper bound for $t \in [t_{s_1}, t_f]$. The same result can be obtained when $\psi_1(t_0) = \psi_0 < 0$. Therefore, (7) is exactly the expression of a^*_{1T}. The proof of Theorem 4.1 is completed. □

Appendix B

Proof of theorem 4.3

The Hamiltonian of player 2 is

$$\begin{aligned} H_2 = {} & \lambda_{21} v_{1x} + \lambda_{22} v_{1y} + \lambda_{23}(a_{1T}\cos\theta_1 - a_{1N}\sin\theta_1) \\ & + \lambda_{24}(a_{1T}\sin\theta_1 + a_{1N}\cos\theta_1) \\ & + \lambda_{25} v_{2x} + \lambda_{26} v_{2y} + \lambda_{27}(a_{2T}\cos\theta_2 - a_{2N}\sin\theta_2) \\ & + \lambda_{28}(a_{2T}\sin\theta_2 + a_{2N}\cos\theta_2) - 1, \end{aligned} \tag{B.1}$$

where $\lambda_{2k}, k = 1, \ldots, 8$ represent the components of co-state of player 2, i.e. λ_2. Denote $f_2(t) = \lambda_{27}\cos\theta_2 + \lambda_{28}\sin\theta_2$ and $g_2(t) = -\lambda_{27}\sin\theta_2 + \lambda_{28}\cos\theta_2$ as the coefficients of a_{2T} and a_{2N} in H_2, respectively. According to (5), one can obtain that if $f_2(t) > 0$, then $a^*_{2T}(t)$ takes value at the upper bound of (3); if $f_2(t) < 0$, then $a^*_{2T}(t)$ takes value at the lower bound of (3). $a^*_{2N}(t)$ have similar results about $g_2(t)$.

Note that (B.1) has the similar form with (A.1). Thus the derivative of λ_{1k} and λ_{2k}, $k = 1, 2, \ldots, 8$, has similar form except for different terminal conditions. Specifically,

$$\begin{aligned} \lambda_{25}(t_f) &= -\mu \frac{\partial \varphi_2(t_f)}{\partial x_2} = -\mu \frac{\partial}{\partial x_2}\left(\arctan\frac{y_1 - y_2}{x_1 - x_2}\right)\Bigg|_{t=t_f} \\ &= -\frac{\mu}{d(t_f)}\sin\alpha_2(t_f), \end{aligned} \tag{B.2}$$

$$\lambda_{26}(t_f) = -\mu \frac{\partial \varphi_2(t_f)}{\partial y_2} = \frac{\mu}{d(t_f)}\cos\alpha_2(t_f), \tag{B.3}$$

$$\begin{aligned} \lambda_{27}(t_f) &= -\mu \frac{\partial \varphi_2(t_f)}{\partial v_{2x}} = -\mu \frac{\partial}{\partial v_{2x}}\left(-\arctan\frac{v_{2y}}{v_{2x}}\right)\Bigg|_{t=t_f} \\ &= -\frac{\mu}{v_2(t_f)}\sin\theta_2(t_f), \end{aligned} \tag{B.4}$$

$$\lambda_{28}(t_f) = -\mu \frac{\partial \varphi_2(t_f)}{\partial v_{2y}} = \frac{\mu}{v_2(t_f)}\cos\theta_2(t_f), \tag{B.5}$$

$$\begin{aligned} \lambda_{21}(t_f) &= \frac{\mu}{d(t_f)}\sin\alpha_1(t_f), \lambda_{22}(t_f) \\ &= -\frac{\mu}{d(t_f)}\cos\alpha_1(t_f), \end{aligned} \tag{B.6}$$

$$\lambda_{23}(t_f) = \lambda_{24}(t_f) = 0, \tag{B.7}$$

where μ is an undetermined constant. It can be proved that

$$\begin{aligned} \lambda_{25} &\equiv -\frac{\mu}{d(t_f)}\sin\alpha_2(t_f), \quad \lambda_{26} \equiv \frac{\mu}{d(t_f)}\cos\alpha_2(t_f), \\ \dot{\lambda}_{27} &= \frac{\mu}{d(t_f)}\sin\alpha_2(t_f) - (\lambda_{27}a_{2T} + \lambda_{28}a_{2N})\sin^2\theta_2 \frac{1}{v_2} \\ &\quad + (-\lambda_{27}a_{2N} + \lambda_{28}a_{2T})\cos\theta_2\sin\theta_2 \frac{1}{v_2}, \\ \dot{\lambda}_{28} &= -\frac{\mu}{d(t_f)}\cos\alpha_2(t_f) + (\lambda_{27}a_{2T} + \lambda_{28}a_{2N})\cos\theta_2 \\ &\quad \times \sin\theta_2 \frac{1}{v_2} - (-\lambda_{27}a_{2N} + \lambda_{28}a_{2T})\cos^2\theta_2 \frac{1}{v_2}, \end{aligned} \tag{B.8}$$

$$\begin{cases} \dot{f}_2 = -\dfrac{\mu}{d(t_f)}\sin(\theta_2 - \alpha_2(t_f)) + g_2(t)\dfrac{a_{2N}}{v_2}, \\ f_2(t_f) = 0, \end{cases} \tag{B.9}$$

$$\begin{cases} \dot{g}_2 = -\dfrac{\mu}{d(t_f)}\cos(\theta_2 - \alpha_2(t_f)) - g_2(t)\dfrac{a_{2T}}{v_2}, \\ g_2(t_f) = \mu / v_2(t_f). \end{cases} \tag{B.10}$$

Besides, owing to the terminal time is free, $H_2(t_f) = 0$. By substituting (B.2)–(B.7) into $H_2(t_f) = 0$, it yields that $\mu \neq 0$. Denote

$$p(t) \triangleq \exp\left(\int_t^{t_f} \frac{a_{2T}(\tau)}{v_2(\tau)}d\tau\right).$$

Obviously $p(t)$ satisfies $p(t) > 0$ and

$$\max\left\{p(t), \frac{1}{p(t)}\right\} < \exp\left((t_f - t)\frac{A_{2T}}{\underline{v}_2}\right). \tag{B.11}$$

Note that (B.10) is a first-order linear ordinary differential equations. Thus

$$g_2(t) = p(t)\left[C + \frac{\mu}{d(t_f)}\int_t^{t_f}\cos(\theta_2(\tau) - \alpha_2(t_f))\frac{1}{p(\tau)}d\tau\right] \tag{B.12}$$

and we have $C = \mu/v_2(t_f)$ when $t = t_f$.

In order to obtain the sign of $g_2(t)$, consider the following inequality:

$$\begin{aligned}\left|\frac{1}{d(t_f)}\int_t^{t_f}\cos(\theta_2(\tau) - \alpha_2(t_f))\frac{1}{p(\tau)}d\tau\right| &\le \frac{(t_f - t_0)}{d(t_f)}\exp\left((t_f - t)\frac{A_{2T}}{\underline{v}_2}\right)\\ &< \frac{1}{\bar{v}_2} < \frac{1}{v_2(t_f)},\end{aligned} \tag{B.13}$$

where the penultimate inequality sign holds because of (9). As a result, the sign of $g_2(t)$ is the same with μ since $v_2(t_f) > 0$, $p(t) > 0$, which means a_{2N}^* has no switching time due to $\mu \neq 0$ and thus $a_{2N}^*(t) \equiv \bar{a}_{2N}$ or $a_{2N}^*(t) \equiv -\bar{a}_{2N}$.

From the first result of Lemma D.1 and (9), one can obtain similarly to the third step of the proof of Theorem 4.1 that under the distance condition (9), $a_{2N}(t) \equiv \bar{a}_{2N}$ decreases $|\eta_2(t_0)|$ to $\eta_2(t) = 0$ faster than $a_{2N}(t) \equiv -\bar{a}_{2N}$ if $\eta_2(t_0) > 0$; $a_{2N}(t) \equiv -\bar{a}_{2N}$ decreases $|\eta_2(t_0)|$ to $\eta_2(t) = 0$ faster than $a_{2N}(t) \equiv \bar{a}_{2N}$ if $\eta_2(t_0) < 0$; Therefore, $a_{2N}^*(t) = \mathrm{sign}(\eta_2(t_0))\bar{a}_{2N}$.

Consider (B.9). By substituting (B.12) into (B.9), one can obtain that

$$\begin{aligned}\dot{f}_2 &= -\frac{\mu}{d(t_f)}\sin(\theta_2 - \alpha_2(t_f)) + \frac{\mu a_{2N}^*}{v_2}p(t)\left[\frac{1}{v_2(t_f)}\right.\\ &\quad\left. + \frac{1}{d(t_f)}\int_t^{t_f}\cos(\theta_2(\tau) - \alpha_2(t_f))\frac{1}{p(\tau)}d\tau\right]\\ &= \frac{\mu}{v_2(t_f)}\frac{a_{2N}^*}{v_2}p(t) + \frac{\mu}{d(t_f)}\left[-\sin(\theta_2 - \alpha_2(t_f))\right.\\ &\quad\left. + \frac{a_{2N}^*}{v_2}p(t)\int_t^{t_f}\cos(\theta_2(\tau) - \alpha_2(t_f))\frac{1}{p(\tau)}d\tau\right].\end{aligned}$$

In order to obtain the sign of $\dot{f}_2$, let $\dot{f}_2$ be multiplied by $v_2/(a_{2N}^* p(t))$. We have

$$\begin{aligned}\frac{\dot{f}_2 v_2}{a_{2N}^* p(t)} &= \frac{\mu}{v_2(t_f)} + \frac{\mu}{d(t_f)}\left[-\frac{\sin(\theta_2 - \alpha_2(t_f))}{p(t)}\frac{v_2}{a_{2N}^*}\right.\\ &\quad\left. + \int_t^{t_f}\cos(\theta_2(\tau) - \alpha_2(t_f))\frac{1}{p(\tau)}d\tau\right]\\ &\triangleq \frac{\mu}{v_2(t_f)} + \mu q(t).\end{aligned} \tag{B.14}$$

Note that (B.11) and

$$\left|\int_t^{t_f}\cos(\theta_2(\tau) - \alpha_2(t_f))d\tau\right| \le (t_f - t).$$

As a result,

$$\begin{aligned}|q(t)| &< \left|\frac{1}{d(t_f)}\exp\left((t_f - t)\frac{A_{2T}}{\underline{v}_2}\right)\left[\frac{\bar{v}_2}{\bar{a}_{2N}} + (t_f - t)\right]\right|\\ &< \left|\frac{1}{d(t_f)}\exp\left((t_f - t)\frac{A_{2T}}{\underline{v}_2}\right)\left(\frac{\bar{v}_2}{\bar{a}_{2N}} + (t_f - t)\right)\right|\\ &< \frac{1}{v_2(t_f)},\end{aligned} \tag{B.15}$$

where the last inequality sign holds because of (9). Equations (B.14) and (B.15) indicate that the sign of $\dot{f}_2$ is the same with μa_{2N}^*. From (B.12) and (B.13), it is clear that the sign of μ is the same with $g_2(t)$, so is a_{2N}^*. As a result, $\mu a_{2N}^* > 0$ and $\dot{f}_2 > 0$. Note that $f_2(t_f) = 0$. Then we have $f_2(t) < 0$ for $t \in [t_0, t_f)$, which means a_{2T}^* takes value at the lower bound of (3). The proof of Theorem 4.3 is completed. □

Appendix C

Lemma C.1 and its proof

Suppose there exist two strategies of player 1. The corresponding trajectories are denoted by $X_1(t)$ and $X_1'(t)$. The corresponding TTAs are $\psi_1(t)$ and $\psi_1'(t)$. The corresponding distances between player 1 and $(x_2(t_f), y_2(t_f))$ are $\bar{d}_{12}(t)$ and $\bar{d}'_{12}(t)$, respectively. Suppose $X_1(t)$ and $X_1'(t)$ have the same speed and $\bar{d}_{12}(t_0) = \bar{d}'_{12}(t_0)$. The following lemma reveals the relationship between distance and TTA. Player 2 has a similar result.

Lemma C.1. *If $|\psi_1(t)| \le |\psi_1'(t)|$ holds for $t \in [t_0, t_f]$, then $\bar{d}_{12}(t) \le \bar{d}'_{12}(t)$ holds for $t \in [t_0, t_f]$.*

Proof. Discretize the time interval with δ_t. Then one can obtain a series of discrete times $t_k = t_0 + k\delta_t$, $k = 0, 1, 2, \ldots$ Suppose the lemma holds at the discrete times $t_0, t_1, \ldots, t_k$, i.e. $|\psi_1(t_n)| \le |\psi_1'(t_n)|$ and thus $\bar{d}_{12}(t_n) \le \bar{d}'_{12}(t_n)$, $n = 1, 2, \ldots, k$. Figure C.1 illustrates the discrete case at t_k.

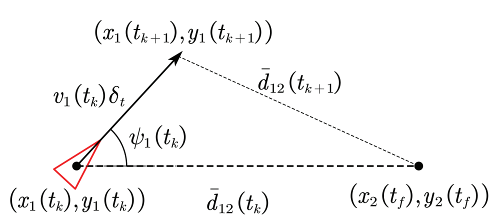

Fig. C.1. The discrete case at t_k.

Then, one can get

$$\bar{d}_{12}(t_{k+1})^2 = \bar{d}_{12}(t_k)^2 + v_1(t_k)^2\delta_t^2 \\ - 2\cos\psi_1(t_k)\,\bar{d}_{12}(t_k)v_1(t_k)\delta_t. \quad (C.1)$$

$\bar{d}'_{12}$ satisfies a similar equation. Consequently, if $|\psi_1(t_k)| \leq |\psi'_1(t_k)|$ and $\bar{d}_{12}(t_k) \leq \bar{d}'_{12}(t_k)$, then $\bar{d}_{12}(t_{k+1}) \leq \bar{d}'_{12}(t_{k+1})$. Let $\delta_t \to 0$ and the proof is completed. □

Lemma C.1 implies that if there exists a strategy which maximizes (minimizes) $|\psi_i|$ during $[t_0, t_f]$, then this strategy can maximizes (minimizes) $d(t_f)$.

Appendix D

Lemma D.1 and its proof

Note that $\dot{\psi}_i = \dot{\beta}_i - \dot{\theta}_i$, $\dot{\varphi}_i = \dot{\alpha}_i - \dot{\theta}_i$. Lemma D.1 explains the properties of $\dot{\alpha}_i$ and $\dot{\beta}_i$.

Lemma D.1. *For any $\varepsilon > 0$,*

(1) *if $d > \sqrt{2}(\bar{v}_1 + \bar{v}_2)/\varepsilon$, then $|\dot{\alpha}_i| < \varepsilon$;*
(2) *if $\bar{d}_{ij} > \bar{v}_i/\varepsilon$, then $|\dot{\beta}_i| < \varepsilon$.*

Proof. One can obtain

$$\begin{aligned}\dot{\alpha}_i &= \frac{\partial}{\partial t}\left(\arctan\frac{y_j(t) - y_i(t)}{x_j(t) - x_i(t)}\right) \\ &= \frac{1}{d^2}\left[(v_{jy} - v_{iy})(x_j - x_i) - (v_{jx} - v_{ix})(y_j - y_i)\right] \\ &= \frac{1}{d}\left[(v_{jy} - v_{iy})\cos\alpha_i - (v_{jx} - v_{ix})\sin\alpha_i\right], \quad (D.1)\end{aligned}$$

$$\begin{aligned}\dot{\beta}_i &= \frac{\partial}{\partial t}\left(\arctan\frac{y_j(t_f) - y_i(t)}{x_j(t_f) - x_i(t)}\right) \\ &= \frac{1}{\bar{d}_{ij}^2}\left[-v_{iy}(x_j(t_f) - x_i) + v_{ix}(y_j(t_f) - y_i)\right] \\ &= \frac{1}{\bar{d}_{ij}}\left[-v_{iy}\cos\beta_i + v_{ix}\sin\beta_i\right]. \quad (D.2)\end{aligned}$$

The first conclusion of Lemma D.1 derives from

$$\max\{|v_{jx} - v_{ix}|, |v_{jy} - v_{iy}|\} < \bar{v}_1 + \bar{v}_2$$

and (D.1). The second conclusion of Lemma D.1 comes from $v_{iy} = v_i\sin\theta_i$, $v_{ix} = v_i\cos\theta_i$ and (D.2). □

Lemma D.1 indicates that $\dot{\alpha}_i \to 0$ when $d \to \infty$ and $\dot{\beta}_i \to 0$ when $\bar{d}_{ij} \to \infty$.

Appendix E

Proof of proposition 5.1

Due to $\psi_i(t) - \varphi_i(t) = \beta_i(t) - \alpha_i(t)$, one needs to consider the error between $\beta_i(t)$ and $\alpha_i(t)$. Figure E.1 demonstrates

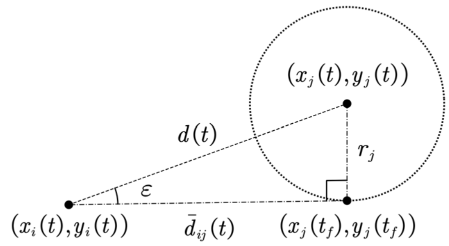

Fig. E.1. The illustration of $|\beta_i(t) - \alpha_i(t)|$.

the case that $\beta_i(t)$ and $\alpha_i(t)$ have the largest difference under the condition $d(t) \geq \bar{v}_j(t_f - t)$, where the circle represents the maximum movement range of player j, $r_j = \bar{v}_j(t_f - t)$ represents the radius of the circle and $\varepsilon \geq |\beta_i(t) - \alpha_i(t)|$. It can be obtained that

$$\varepsilon = \arcsin\frac{r_j}{d(t)} = \arcsin\frac{\bar{v}_j(t_f - t)}{d(t)}. \quad (E.1)$$

Thus

$$|\psi_i(t) - \varphi_i(t)| \leq \left|\arcsin\frac{\bar{v}_j(t_f - t)}{d(t)}\right|. \quad (E.2)$$

□

ORCID

Zinxin Feng https://orcid.org/0000-0003-4830-8066
Wenchao Xue https://orcid.org/0000-0003-0637-9413
Hongsheng Qi https://orcid.org/0000-0002-1698-7570
Long Cheng https://orcid.org/0000-0001-7565-8788

References

[1] X. Liu, S. Li and M. Xin, Mars entry trajectory planning with range discretization and successive convexification, *J. Guid. Control Dyn.* **45**(4) (2022) 755–763.
[2] X. Yan and L. He, Unpowered approach and landing trajectory planning using second-order cone programming, *Aerosp. Sci. Technol.* **101** (2020) 105841.
[3] Y. Liu, B. Zhou, X. Wang, L. Li, S. Cheng, Z. Chen, G. Li and L. Zhang, Dynamic lane-changing trajectory planning for autonomous vehicles based on discrete global trajectory, *IEEE Trans. Intell. Transp. Syst.* **23**(7) (2021) 8513–8527.
[4] S. Li, Z. Li, Z. Yu, B. Zhang and N. Zhang, Dynamic trajectory planning and tracking for autonomous vehicle with obstacle avoidance based on model predictive control, *IEEE Access* **7** (2019) 132074–132086.
[5] Á. Madridano, A. Al-Kaff, D. Martín and A. de la Escalera, Trajectory planning for multi-robot systems: Methods and applications, *Expert Syst. Appl.* **173** (2021) 114660.
[6] S. M. LaValle, Robot motion planning: A game-theoretic foundation, *Algorithmica* **26**(3) (2000) 430–465.
[7] F. Christ, A. Wischnewski, A. Heilmeier and B. Lohmann, Time-optimal trajectory planning for a race car considering variable tyre-road friction coefficients, *Veh. Syst. Dyn.* **59**(4) (2021) 588–612.

[8] Y. Huang, H. Ding, Y. Zhang, H. Wang, D. Cao, N. Xu and C. Hu, A motion planning and tracking framework for autonomous vehicles based on artificial potential field elaborated resistance network approach, *IEEE Trans. Ind. Electron.* **67**(2) (2019) 1376–1386.
[9] Y. Liu, C. Guo and Y. Weng, Online time-optimal trajectory planning for robotic manipulators using adaptive elite genetic algorithm with singularity avoidance, *IEEE Access* **7** (2019) 146301–146308.
[10] D. Delahaye, S. Chaimatanan and M. Mongeau, Simulated annealing: From basics to applications, in *Handbook of Metaheuristics* (2019), pp. 1–35.
[11] A. Friedman, *Differential Games* (Courier Corporation, 2013).
[12] M. H. Breitner, H. J. Pesch and W. Grimm, Complex differential games of pursuit-evasion type with state constraints, part 1: Necessary conditions for optimal open-loop strategies, *J. Optim. Theory Appl.* **78**(3) (1993) 419–441.
[13] J. Shinar and V. Turetsky, Missile guidance laws based on pursuit-evasion game formulations, *IFAC Proc. Vol.* (2001).
[14] X. Li, Z. Peng, W. Zha and J. Chen, Construction of barrier in a three-player pursuit-evasion game, *Unmanned Syst.* **4**(01) (2016) 41–49.
[15] H. Fu and H. H. Liu, Optimal solution of a target defense game with two defenders and a faster intrude, *Unmanned Syst.* **09**(03) (2021) 247–262.
[16] A. Jagat and A. J. Sinclair, Nonlinear control for spacecraft pursuit-evasion game using the state-dependent riccati equation method, *IEEE Trans. Aerosp. Electron. Syst.* **53**(6) (2017) 3032–3042.
[17] W. Lin, Z. Qu and M. A. Simaan, Nash strategies for pursuit-evasion differential games involving limited observations, *IEEE Trans. Aerosp. Electron. Syst.* **51**(2) (2015) 1347–1356.
[18] V. Turetsky and T. Shima, Pursuit-evasion guidance in a switched system, *SIAM J. Control Optim.* **56**(4) (2018) 2613–2633.
[19] X. Tang, D. Ye, L. Huang, Z. Sun and J. Sun, Pursuit-evasion game switching strategies for spacecraft with incomplete-information, *Aerosp. Sci. Technol.* **119** (2021) 107112.
[20] E. Garcia, D. W. Casbeer, A. Von Moll and M. Pachter, Multiple pursuer multiple evader differential games, *IEEE Trans. Autom. Control* **66**(5) (2020) 2345–2350.
[21] Z. Zhou, J. R. Shewchuk, D. Stipanović, H. Huang and C. J. Tomlin, Smarter lions: Efficient cooperative pursuit in general bounded arenas, *SIAM J. Control Optim.* **58**(2) (2020) 1229–1256.
[22] V. G. Lopez, F. L. Lewis, Y. Wan, E. N. Sanchez and L. Fan, Solutions for multiagent pursuit-evasion games on communication graphs: Finite-time capture and asymptotic behaviors, *IEEE Trans. Autom. Control* **65**(5) (2019) 1911–1923.
[23] Y. Wang, L. Dong and C. Sun, Cooperative control for multi-player pursuit-evasion games with reinforcement learning, *Neurocomputing* **412** (2020) 101–114.
[24] W. Lu, H. Liu and Q. Gao, Data-driven cooperative multi-task assignment in heterogeneous multi-agent pursuit-evade game, *Unmanned Syst.* **12**(03) (2024) 523–533.
[25] B. Lian, V. S. Donge, F. L. Lewis, T. Chai and A. Davoudi, Data-driven inverse reinforcement learning control for linear multiplayer games, *IEEE Trans. Neural Netw. Learn. Syst.* **35**(2) (2022) 2028–2041.
[26] M. Chen, Z. Zhou and C. J. Tomlin, Multiplayer reach-avoid games via pairwise outcomes, *IEEE Trans. Autom. Control* **62**(3) (2016) 1451–1457.
[27] M. H. Breitner, H. J. Pesch and W. Grimm, Complex differential games of pursuit-evasion type with state constraints, part 2: Numerical computation of optimal open-loop strategies, *J. Optim. Theory Appl.* **78**(3) (1993) 443–463.
[28] Z. Nikooeinejad, A. Delavarkhalafi and M. Heydari, A numerical solution of open-loop Nash equilibrium in nonlinear differential games based on Chebyshev pseudospectral method, *J. Comput. Appl. Math.* **300** (2016) 369–384.
[29] A. W. Starr and Y. C. Ho, Nonzero-sum differential games, *J. Optim. Theory Appl.* **3**(3) (1969) 184–206.
[30] J. H. Case, Equilibrium points of n-person differential games, Technical Report, Michigan University, Ann Arbor (1967) 6717740.

Zixin Feng received his bachelor degree from Zhengzhou University in 2018 and received his master degree from University of Chinese Academy of Sciences in 2022. He is now an Ph.D. candidate at the School of Mathematical Sciences, University of Chinese Academy of Sciences. His research interest covers optimal control, games and their application in trajectory planning and distributed decision.

Wenchao Xue received the B.S. degree in applied mathematics from Nankai University, Tianjin, China, in 2007, and the Ph.D. degree in control theory from the Academy of Mathematics and Systems Science, Chinese Academy of Sciences, Beijing, China, in 2012.

He is currently an Professor with the Key Laboratory of Systems and Control, Academy of Mathematics and Systems Science, Chinese Academy of Sciences. His research interests include active disturbance rejection control, and filter design for nonlinear uncertain systems.

Hongsheng Qi received the Ph.D. degree in systems theory from the Academy of Mathematics and Systems Science, Chinese Academy of Sciences, Beijing, China, in 2008.

From July 2008 to May 2010, he was a Postdoctoral Fellow with the Key Laboratory of Systems Control, Chinese Academy of Sciences. He is currently an Professor with Academy of Mathematics and Systems Science, Chinese Academy of Sciences. His research interests include logical dynamic systems, game theory, quantum networks, etc.

Dr. Qi was a recipient of "Automatica" 2008–2011 Theory/Methodology Best Paper Prize in 2011 and a recipient of a second National Natural Science Award of China in 2014.

Long Cheng received the B.S. degree (Hons.) in control engineering from Nankai University, Tianjin, China, in 2004, and the Ph.D. degree (Hons.) in control theory and control engineering from the Institute of Automation, Chinese Academy of Sciences, Beijing, China, in 2009. He is currently a Professor with the State Key Laboratory of Multimodal Artificial Intelligence Systems, Institute of Automation, Chinese Academy of Sciences. He is also a Professor with the University of Chinese Academy of Sciences, Beijing. He has published more than 100 technical papers in peer-refereed journals and prestigious conference proceedings. His research interests include rehabilitation robot, intelligent control, and neural networks.

Dr. Cheng was a recipient of IEEE Transactions on Neural Networks Outstanding Paper Award from the IEEE Computational Intelligence Society, the Aharon Katzir Young Investigator Award from the International Neural Networks Society, and the Young Researcher Award from the Asian Pacific Neural Networks Society. He is an Associate Editor of IEEE Transactions on Cybernetics, IEEE Transactions on Automation Science and Engineering, Science China Technological Sciences, and Acta Automatica Sinica.